Bottom quark mass prediction in supersymmetric grand unification: Uncertainties and constraints

Paul Langacker and Nir Polonsky
Department of Physics, University of Pennyslvania, Philadelphia, Pennsylvania 19104
(Received 4 June 1993)

Grand unified theories often predict unification of Yukawa couplings (e.g., $h_b = h_\tau$), and thus certain relations among fermion masses. The latter can distinguish these from models that predict only coupling constant unification. The implications of Yukawa couplings of the heavy family in the supersymmetric extension of the standard model (when embedded in a GUT) are discussed. In particular, uncertainties associated with m_t and m_b, threshold corrections at the low-scale, and threshold and nonrenormalizable-operator corrections associated with a grand-unified sector at the high-scale are parametrized and estimated. The implications of these and of the correlation between m_t and the prediction for α_s are discussed. Constraints on the $\tan\beta$ range in such models and an upper bound on the t-quark pole mass are given and are shown to be affected by the α_s-m_t correlation. Constraints on the low-scale thresholds are found to be weakened by uncertainties associated with the high scale.

PACS number(s): 12.10.Dm, 11.30.Pb, 12.15.Ff

I. INTRODUCTION

Recent CERN e^+e^- collider LEP [1] and other precision electroweak data are known [2] to be consistent with coupling constant unification within the minimal supersymmetric standard model (MSSM) [3], in which the standard model (SM) matter is minimally extended, i.e., the Higgs sector contains one pair of Higgs doublets and there is a grand desert (up to small perturbations) between the weak (low) and unification (high) scales. Recently, it was further shown [4] that corrections associated with the t quark and Higgs scalar thresholds, sparticle spectrum (for example, see Ref. [5]), Yukawa couplings, a possible embedding of the MSSM in a grand unified theory (GUT) [6], and nonrenormalizable effects [7], as well as constraints [8,9] from proton decay nonobservation [10], introduce theoretical uncertainties but do not alter the successful unification; e.g., the prediction of $\alpha_s(M_Z) \approx 0.125 \pm 0.010$ [4] agrees well with the observed value. Such uncertainties depend on seven different effective parameters in addition to the t-quark mass and Yukawa coupling. [The ± 0.010 is a sum (in quadrature) of the different theoretical uncertainties estimated using reasonable ranges for the various parameters.] This theoretical uncertainty is sufficiently large that few meaningful constraints can be derived from the $\alpha_s(M_Z)$ prediction by itself. Similar conclusions were reached by Barbieri, Hall, and Sarid [11].

If, indeed, coupling constant unification is a hint for a supersymmetric (SUSY) GUT, then a next step is to study the predicted relationships among fermion masses in such theories [12], in a way that consistently incorporates the different theoretical uncertainties listed above. (The nature of the theoretical corrections, and in particular the presence of adjoint representations, also distinguishes such models from many string-inspired ones.) Let us assume in the following (in addition to the MSSM) that we have (i) coupling constant unification, and (ii) third-family two-Yukawa unification. That is, at the unification point M_G (the point above which all the GUT gauge group supermultiplets are complete) we have $h_b(M_G) = h_\tau(M_G)$, as is the case [12] in a minimal SU(5) unification, which we will assume below for definiteness, and in similar unification schemes.[1] h_α is the MSSM Yukawa coupling of a fermion of type α and $M_G \approx 10^{16} - 10^{17}$ GeV.

Assumption (ii) can be incorporated into more ambitious attempts [13] to explain the origin of all fermion masses. Such models, which assume extended high-scale structures ("textures"), were shown recently [14–20] to have successful predictions as well as possible implications for neutrino masses. However, limiting our analysis to assumptions (i) and (ii), we neglect hereafter the Yukawa couplings of the first two families (where empirically $m_d/m_s \approx 10 m_e/m_\mu$, rather than $m_d/m_s \approx m_e/m_\mu$; the latter would be implied by extending assumption (ii) to the first two families and their negligibly small Yukawa couplings) and also flavor mixings. The usual argument goes that some perturbation modifies the couplings or masses of the first two families[2] without significantly altering (ii). We do not elaborate on any such mechanism. A special case of (ii) is a third-family three-Yukawa unification, i.e., $h_t(M_G) = h_b(M_G) = h_\tau(M_G)$, which is the situation in some SO(10) models involving a single complex Higgs 10-plet. We will consider such a possibility as well.

[1] This holds in models such as SU(5), SO(10) and E_6 for the Yukawa coupling of Higgs fields in the fundamental (5, 10, 27) representations.

[2] In the texture models mentioned above, such a mechanism is realized by introducing large Higgs representations [e.g., 45 of SU(5) or 126 and 210 of SO(10)] and (in most cases) a set of flavor symmetries. For a different possibility involving nonrenormalizable operators, see Ref. [21].

Let us stress that we do not take (ii) to be independent of (i). The coupling constant unification assumption by itself is not enough to significantly constrain the MSSM parameter space. Here, we examine whether more can be said when imposing (ii) as an additional assumption that can possibly distinguish GUT models from some GUT-like string-inspired models [where (ii) is not expected to hold in general]. Assumption (ii) was considered recently by several groups. Some [22], either (a) carried out a one-loop analysis, (b) assumed a low $\alpha_s(M_Z)$ [e.g., $\alpha_s(M_Z)\sim 0.11$, which is lower than the value expected from coupling constant unification] as an input, (c) ignored the correlation between m_t and the predicted value of $\alpha_s(M_Z)$, and/or (d) allowed the running b-quark mass m_b to be as high as 5 GeV (which, as we discuss below, is a more appropriate upper bound on the pole mass). More recent results of two-loop analyses [5,18,23] imply a very constrained parameter space, i.e., only a small allowed area in the $m_t^{\rm pole}$-tanβ plane, where $m_t^{\rm pole}$ is the t-quark pole mass and tanβ is the ratio of the two Higgs doublet expectation values, $v_{h_{\rm up}}/v_{h_{\rm down}}$. Therefore, one would hope that linking (i) with (ii) (and considering uncertainties associated with m_t and m_b) will result in some useful constraints on the MSSM parameters, assuming a minimal SU(5)-type unification (for example, see Ref. [5]).

Below, we carry out a careful analysis under the above assumptions and consider various theoretical uncertainties in the calculation. We find that requiring (i) and predicting $\alpha_s(M_Z)$ as a function of $m_t^{\rm pole}$ and of tanβ [4] in the range of ~ 0.12–0.13 (see Fig. 1), constrains the tanβ range allowed by (ii) more severely than suggested by previous analyses. On the other hand, various theoretical uncertainties can relax the constraints. We also obtain ~ 215 GeV for the upper bound on $m_t^{\rm pole}$ (where α_s-m_t correlations were taken into account). Some information about the low-scale mass parameters can be extracted. However, corrections associated with the high scale contribute significantly to the theoretical uncertainties and weaken any constraints. The only spectrum parameter that is strongly constrained is tanβ. In agreement with other authors, we find low- (~ 0.6–3) and high- (~ 40–58) tanβ allowed regions (branches). The former saturates the h_t infrared fixed-point [24] line (the divergence line). The $\alpha_s - m_t$ correlation modifies the fixed point value for h_t and diminishes the dependence of the allowed tanβ range on $m_t^{\rm pole} \lesssim 215$ GeV. Theoretical uncertainties (and in particular, those associated with the high scale) determine the width of each branch and, thus, the separation between the two branches.

The various data (and, in particular, the b-quark mass) and the procedure are reviewed in Sec. II. The constraints on the $m_t^{\rm pole}$-tanβ plane and the role of the strong coupling are presented and discussed in Sec. III. The different correction terms are described and evaluated in greater detail in Sec. IV. We summarize our conclusions in Sec. V. Throughout this work we keep the philosophy (and where relevant, the notation) we introduced previously [4].

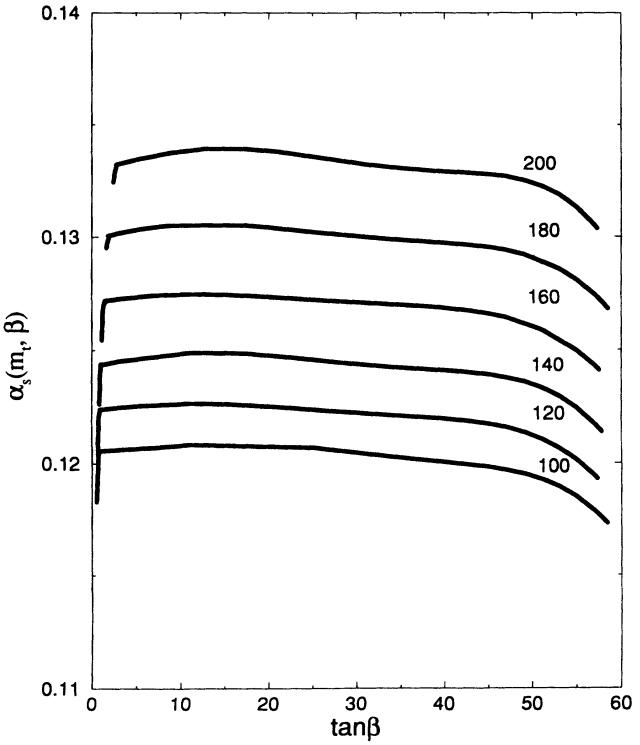

FIG. 1. The predicted strong coupling at the Z pole, $\alpha_s(M_Z)$, for different values of the t-quark pole mass $m_t^{\rm pole}$, and of the two Higgs doublet expectation value ratio, tanβ. $h_b(M_G)=h_\tau(M_G)$ is assumed. $m_t^{\rm pole}$ (in GeV) is indicated on the right-hand side above the relevant line.

II. INPUT DATA AND PROCEDURE

At the Z pole,

$$M_Z = 91.187 \pm 0.007 \text{ GeV} , \tag{1}$$

and using the modified minimal subtraction scheme ($\overline{\rm MS}$) [25] the weak angle and couplings[3] are [4,26,27]

$$s^2(M_Z) = 0.2324 - 1.03\times 10^{-7}[m_t^{\rm pole}({\rm GeV})^2 - (138)^2] \pm 0.0003 , \tag{2}$$

$$\frac{1}{\alpha(M_Z)} = 127.9 \pm 0.1 , \tag{3}$$

$$\alpha_s(M_Z) = 0.12 \pm 0.01 , \tag{4}$$

where we displayed explicitly the quadratic dependence of $s^2(M_Z)$ on $m_t^{\rm pole}$, which is decoupled from the 0.0003 uncertainty [4]. The $U(1)_{Y/2}$, $SU(2)_L$, and $SU(3)_c$ couplings are given by

[3] A predicted $\alpha_s(M_Z)$ slightly above 0.13, as it is for a heavy enough t quark (see Fig. 1), does not contradict (4); the $\alpha_s(M_Z)$ prediction still has a fairly large theoretical uncertainty of $\sim \pm 0.008$.

$$\frac{1}{\alpha_1(M_Z)}=\frac{3}{5}\frac{1-s^2(M_Z)}{\alpha(M_Z)}\ ,$$

$$\frac{1}{\alpha_2(M_Z)}=\frac{s^2(M_Z)}{\alpha(M_Z)}\ ,$$

and

$$\frac{1}{\alpha_3(M_Z)}=\frac{1}{\alpha_s(M_Z)}\ ,$$

respectively.

For the fermion masses, from electroweak precision data[4] we have, for the t quark [4],

$$m_t^{\rm pole}=138^{+20}_{-25}\pm 5\ {\rm GeV} \tag{5}$$

for a Higgs boson mass in the range 50–150 GeV, which is appropriate for the MSSM. The pole mass is related to the $\overline{\rm MS}$ running mass m_t to leading order[5] in α_s by $m_t=(1-\frac{4}{3}\alpha_s/\pi)m_t^{\rm pole}$. The τ-lepton ($\overline{\rm MS}$ running) mass [31] is given at the Z pole by

$$m_\tau(M_Z)=1.7486\pm 0.0006\ {\rm GeV}\ , \tag{6}$$

which corresponds to (3) and $m_\tau^{\rm pole}=1.7771\pm 0.0005$ GeV [32].

The situation regarding the b-quark mass is more complicated. There are ambiguities in the extraction of the $\overline{\rm MS}$ running mass m_b. Gasser and Leutwyler [33] point out that there is no universal prescription for the relevant scale where α_s is to be evaluated, which suggests that the extraction of m_b is to be carried out case by case, or alternatively, for a range of α_s. (We will adopt the latter.) Gasser and Leutwyler identify (to leading order in α_s) the running mass $m_b(m_b)$ with the Euclidean mass parameter. This point was emphasized by Narison, who offers an alternative definition of $m_b(m_b^{\rm pole})$ [34]. The different definitions introduce a scale ambiguity. Another theoretical difficulty may arise from the role of nonperturbative effects of the interpretation of potential models [33].[6] The next-to-leading correction to the ratio of the $\overline{\rm MS}$ running mass to the pole mass was given more recently by Gray *et al.* [30], i.e.,

$$m_b=m_b^{\rm pole}\left[1-\frac{4}{3}\frac{\alpha_s}{\pi}-12.4\left[\frac{\alpha_s}{\pi}\right]^2\right]\ . \tag{7}$$

The above comments call for some caution, especially given our aim of exploring the strongly constrained $m_t^{\rm pole}$-tanβ plane. Let us then adopt a conservative attitude, i.e.,

$$m_b(5\ {\rm GeV})\le 4.45\ {\rm GeV}\ , \tag{8}$$

which corresponds, for example, to $m_b^{\rm pole}\le 5$ GeV, $\alpha_s\ge 0.17$, and using (7). The next-to-leading correction term in (7) reduces m_b, and $m_b^{\rm pole}\approx 4.5$ GeV, $\alpha_s\gtrsim 0.2$ implies $m_b<4$ GeV. For example, $m_b^{\rm pole}\approx 4.5$ GeV, $\alpha_s\approx 0.25$ gives $m_b\approx 4.0$ GeV when neglecting the next-to-leading term, and $m_b\approx 3.7$ GeV when using (7). The m_b prediction, on the other hand, lies (in general) above 4 GeV. Given the above, we do not specify a lower bound equivalent to (8). Also, requiring $m_b(4.45\ {\rm GeV})\le 4.45$ GeV [which will correspond to $m_b(m_b)=4.25\pm 0.20$ GeV [33], where we have doubled the uncertainty] is somewhat more constraining [e.g., $m_b(4.45\ {\rm GeV})-m_b(5\ {\rm GeV})\approx 0.05-0.15$ GeV—depending on α_s].

We use $\alpha(M_Z)$, $s^2(M_Z)$, and the τ-lepton and t-quark Yukawa couplings,

$$h_\tau(M_Z)=\frac{m_\tau(M_Z)}{174\ {\rm GeV}\cos\beta} \tag{9}$$

and

$$h_t(M_Z)=\left[1-\frac{4}{3}\frac{\alpha_s(M_Z)}{\pi}\right]\frac{m_t^{\rm pole}}{174\ {\rm GeV}\sin\beta}\ , \tag{10}$$

to predict[7] $\alpha_s(M_Z)$ and $h_b(M_Z)$, for a definite point in the $m_t^{\rm pole}$-tanβ plane. One should note that h_t depends on $m_t^{\rm pole}$ also via the $\alpha_s(M_Z)$ correction in (10) (and via the α_3 contribution to the running—see below). As we pointed out, $s^2(M_Z)$ depends quadratically on $m_t^{\rm pole}$. Therefore, we neglect all subleading logarithmic dependencies on $m_t^{\rm pole}$ (for a discussion, see Ref. [4]), including small corrections to (10). We further neglect the error bars in (1)–(3) and in (6). Also, α_i are converted to the dimensional reduction ($\overline{\rm DR}$) scheme, using the proper step functions [35]. Using two-loop renormalization group equations (RGE's) [36] iteratively, we are able to predict $\alpha_s(M_Z)$ and $h_b(M_Z)$ as functions of $m_t^{\rm pole}$ and tanβ. We take $100<m_t^{\rm pole}<200$ GeV as a reasonable conservative range, and constrain tanβ only by requiring the Yukawa couplings to stay perturbative, i.e., $h_\alpha(\mu)<3$ where $M_Z<\mu<M_G$ and $\alpha=t,b,\tau$. (This range can be also justified by requiring two-loop contributions to the RGE's to be less than a quarter of the one-loop ones [18].) We then run down using three-loop QCD and two-loop QED RGE's [31] to find $m_b^0(5\ {\rm GeV})$, where the m_b^0 prediction is that of m_b, but without (theoretical) corrections to the RG calculation.

In any realization of the MSSM, there are small perturbations (order of magnitude of two-loop terms) to the grand desert and unification assumptions, as described above. Thus, in general, $m_b=\rho^{-1}m_b^0$ where $\rho^{-1}\neq 1$ is a correction parameter which incorporates the uncertain-

[4]Slightly more recent data yield [28] $m_t^{\rm pole}=134^{+23}_{-28}\pm 5$ GeV (for $m_{h^0}\sim 60$–150 GeV and including two-loop $\alpha\alpha_s m_t^2$ corrections) and $s^2(M_Z)=0.2326\pm 0.0006$ (m_t free). For our present purposes the difference with (2) and (5) is negligible. The new data will be incorporated in future analysis [29].

[5]The next-to-leading correction [30,31] is $\sim 2\%$ (depending on α_s). The leading correction given here is $\sim 5\%$. (See also the discussion of $m_b/m_b^{\rm pole}$ below.) We neglect the former (together with other subleading m_t and $m_t^{\rm pole}$ effects) while keeping the latter.

[6]The constituent mass parameter in these models is identified with the pole mass.

[7]I.e., case (b) in the notation of Ref. [4].

ties in the running from M_Z up to M_G. Let us stress that in our formulation one does not change the MSSM β functions to those of the SM at m_t or at some other effective scale. Rather, leading m_t^{pole} effects are accounted for in (2), and all other such effects determine ρ^{-1}. A point in the m_t^{pole}-tanβ is excluded if either $h_t > 3$ (tan$\beta \lesssim 1-2$ and/or $m_t^{\text{pole}} \gtrsim 215$ GeV), $h_b (\sim h_\tau) > 3$ (tan$\beta \gtrsim 58$), or

$$m_b(5\text{ GeV}) = \rho^{-1} m_b^0(5\text{ GeV}) > 4.45\text{ GeV} . \quad (11)$$

Incorporating uncertainties associated with m_t^{pole} and Yukawa couplings (in addition to the $\overline{\text{DR}}$ conversion step functions) in the numerical procedure[8] we have to further consider uncertainties associated with the sparticle and Higgs thresholds, high-scale thresholds, and Planck-scale nonrenormalizable operators. For simplicity, we will assume that we have one heavy ($M_H \gg M_Z$) Higgs doublet that decouples with the sparticles, and another light ($m_h \sim M_Z$) SM-like doublet that is responsible for all fermion masses.[9] We are able to obtain an (approximate) analytic expression for ρ^{-1} by expanding one-loop expressions around their unperturbed values. This will be carried out in Sec. IV, where we study the different contributions to ρ^{-1} in GUT models, and estimate ρ^{-1} in the minimal SU(5) model. High-scale corrections to the coupling constant unification (and not the details of the sparticle spectrum) constitute the larger uncertainty. We take

$$\rho^{-1} = 1.00 \pm 0.15 , \quad (12)$$

which is a conservative estimate derived for reasonable ranges of the various correction parameters. Using (12), the exclusion condition (11) reads

$$m_b(5\text{ GeV}) \geq 0.85 m_b^0(5\text{ GeV}) > 4.45\text{ GeV} . \quad (13)$$

III. THE m_t^{pole}-tanβ PLANE

Given the above, we find that assumptions (i) and (ii) allow for a low-tan β branch and a high-tanβ branch. The allowed parameter space is shown in Fig. 2, where the narrow strip corresponding to three-Yukawa unification is also indicated. The low-tanβ branch is shown in greater detail in Fig. 3, where the lines corresponding to $\rho^{-1}=1$ and $h_t(M_G)=2$ are displayed for comparison. The former is, in fact, the h_t infrared fixed-point [24] line, which is the h_t-divergence line. [$h_t(M_Z) > h_t^{\text{fixed}} \Rightarrow h_t(\mu) \gg 1$ for $\mu < M_G$.] This point was also discussed recently in Refs. [18,23]. $\rho^{-1} \neq 1$ only slightly extends the allowed tanβ range. It is also interesting to note that constraints from proton decay via dimension-five operators would exclude the high-tanβ branch for $\rho^{-1} \equiv 1$ (i.e., tan$\beta \lesssim 4.7$ [8]). However, once correction terms are included, M_G can grow significantly [9,4,11] and no useful constraints on tanβ can be derived from proton decay nonobservation [9]. For comparison, we show in Fig. 4 the equivalent parameter space with (13) replaced by $0.85 m_b^0(4.45\text{ GeV}) > 4.45$ GeV. The allowed tanβ range is reduced by $\sim 0.03-0.10$ for the low-tanβ branch and by 3–4 for the high-tanβ one. Replacing (13) with $0.85 m_b^0(\sim 5.1\text{ GeV}) \gtrsim 4.6$ GeV would have a similar but opposite effect (i.e., slightly decreasing the separation between the two branches). A smaller (larger) uncertainty in (12) will have an effect similar to the former (latter). The ρ^{-1}-range estimate (and the m_b upper bound) determine the width of each branch, and thus the excluded intermediate tanβ range. Perturbative consistency (i.e., the divergence lines discussed above) excludes the very small and the very large tanβ ranges and determines the upper bound on m_t^{pole}, $m_t^{\text{pole}} \lesssim 215 \pm 10$

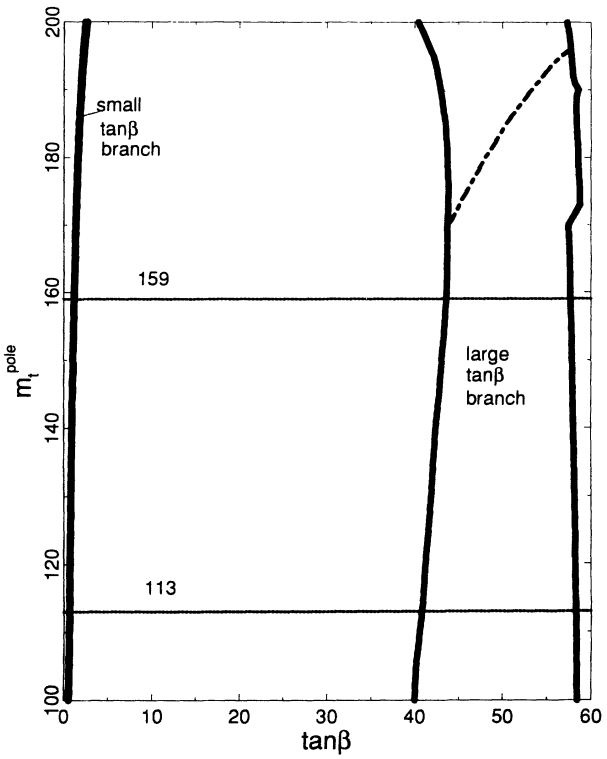

FIG. 2. The m_t^{pole}-tanβ plane is divided into five different regions. Two areas (low- and high-tanβ branches) are consistent with perturbative two-Yukawa coupling unification [$h_b(M_G) = h_\tau(M_G)$] and with $0.85 m_b^0(5\text{ GeV}) < 4.45$ GeV. Between the two branches the b-quark mass is too high. For a too low (high) tanβ, h_t (h_b) diverges. The strip where all three (third-family) Yukawa couplings unify intersects the allowed high-tanβ branch and is indicated as well (dash-dotted line). Corrections to the h_t/h_b ratio induce $a \sim \pm 5\%$ (vertical) uncertainty in the m_t^{pole} range that corresponds to each of the points in the three-Yukawa coupling unification strip. $\alpha_s(M_Z)$, α_G, and the unification scale used in the calculation are the ones predicted by the MSSM coupling constant unification, and are sensitive to the t-quark pole mass, m_t^{pole} (see Fig. 1). The m_t^{pole} range suggested by the electroweak data is indicated (dashed lines) for comparison. m_t^{pole} is in GeV.

[8] In the notation of Ref. [4], $\Delta_i^{\text{conversion}}$, Δ_i^{top}, and Δ_i^{Yukawa}, are all directly incorporated in the calculation.

[9] In such a case, SU(2)-breaking effects are, in general, negligible above m_t.

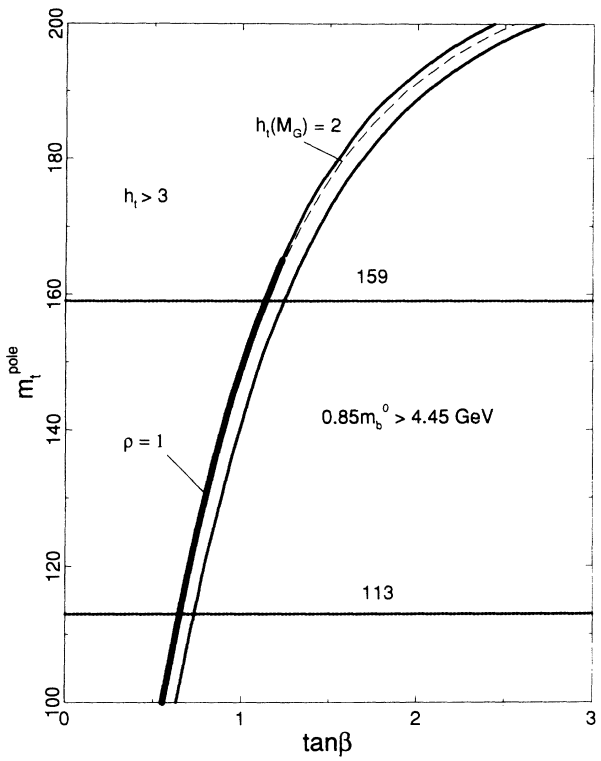

FIG. 3. The low-tanβ branch of Fig. 2 is shown in greater detail. The lines corresponding to $\rho^{-1}=1$ (thick) and $h_t(M_G)=2$ (dashed) are indicated. To the left of the allowed branch one obtains $h_t(M_G)>3$.

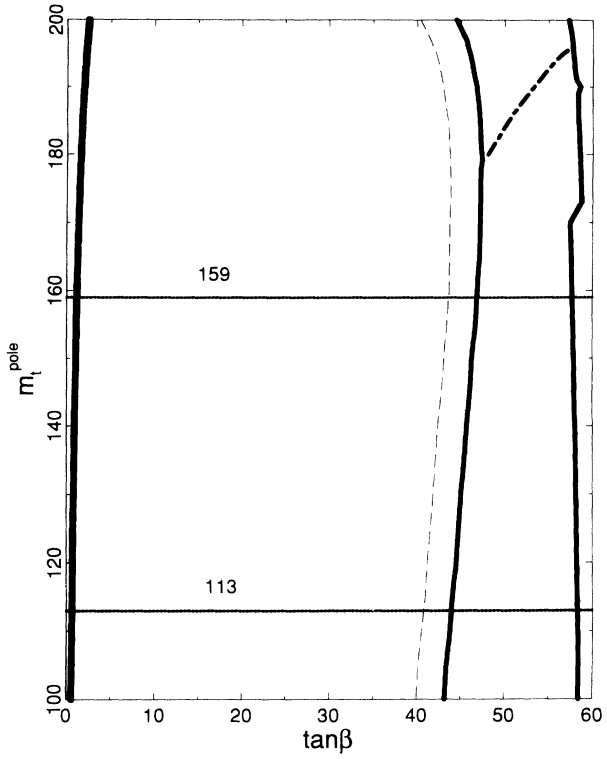

FIG. 4. The same as Fig. 2, except the constraint is replaced with the more restrictive one, $0.85m_b^0(4.45\text{ GeV})<4.45$ GeV. The allowed tanβ range is reduced by $\sim 0.03-0.10$ for the low-tanβ branch (the effect is hardly seen in the figure) and by $\sim 3-4$ for the high-tanβ branch [where the corresponding range for $0.85m_b^0(5\text{ GeV})<4.45$ GeV is indicated—dashed line—for comparison].

GeV, where the ± 10 GeV uncertainty is due to ρ_{top}.

The h_t divergence line eventually becomes approximately parallel to the tanβ axis (and determines the upper bound $m_t^{\text{pole}} \lesssim 215$ GeV). Some intermediate values of tanβ are thus allowed for $m_t^{\text{pole}} > 200$ GeV. (The h_b and h_t divergence lines meet near the $h_b = h_t$ line.) Otherwise, Yukawa unification at the grand unification scale is ruled out[10] if $2.7 \lesssim \tan\beta \lesssim 40$. Furthermore, the low-tanβ branch, where $h_t \sim 1$ and which many would consider a more natural choice, saturates the fixed-point line and has to be adjusted to a few parts in a hundred (a few parts in a thousand, if $\rho^{-1}=1$) for a given m_t^{pole} (see Fig. 3). The large-tanβ branch is more spread and implies, in general, a much lower h_t and $h_t < h_b$. (h_t can still be large for a large enough m_t^{pole}, and $h_t > h_b$ above the three-Yukawa-coupling unification strip.) While we find no constraints on $m_t^{\text{pole}} \lesssim 215$ GeV from two-Yukawa-coupling unification, three-Yukawa-coupling unification is ruled out unless $169 \lesssim m_t^{\text{pole}} \lesssim 196$ GeV. (A slightly larger range, i.e., $m_t^{\text{pole}} \gtrsim 160$ GeV, is allowed when one includes corrections to the h_t/h_b ratio which induce a $\sim 5\%$ theoretical uncertainty. We comment more on this point in Sec. IV.) One expects mutual implications [29] between the above observations and radiative-breaking of SU(2)⊗U(1), an attractive feature of the MSSM that prefers $h_t > h_b$ [38].

To demonstrate the effect of calculating m_b using the predicted $\alpha_s(M_Z)$ rather than a fixed input value, i.e., of associating the Yukawa coupling unification with the rather high values of $\alpha_s(M_Z)$ predicted by $\alpha_1-\alpha_2$ unification, we compare Fig. 2 with Figs. 5–7. There, $\alpha_s(M_Z)$ is fixed [$\alpha_s(M_Z)=0.11$, 0.12, and 0.13, in Figs. 5, 6, and 7, respectively], and thus assumption (i) is relaxed; i.e., for $\alpha_s(M_Z)=0.11(0.12,0.13)$ there is a $\sim 7\%$ ($\sim 3\%$) split between $\alpha_3(M_G)$ and the α_G defined by α_1 and α_2. Let us stress that the different corrections are not treated on equal footing in this case, because some are included in ρ^{-1} while others [such as nonrenormalizable operators (NRO's)] are absorbed in the fixed value of $\alpha_s(M_Z)$. Furthermore, the appropriateness of this decomposition depends on which type of uncertainties shift the predicted $\alpha_s(M_Z)$. (We elaborate more on this point in Sec. IV.) Nevertheless, the comparison illustrates that a low $\alpha_s(M_Z)$ is preferred by m_b. The allowed parameter space for $\alpha_s(M_Z)=0.11$ (Fig. 5) is much larger than that for $\alpha_s(M_Z)=0.13$ (Fig. 7). For a lower value of α_s the radiative corrections that reduce h_b are dimin-

[10]For a large tanβ ($v_{h_{\text{down}}} \ll v_{h_{\text{up}}}, v$) some caution may be required regarding the scale at which the Higgs potential is minimized and tanβ is defined, as was pointed out by Bando *et al.* [22] and by Chankowski [37].

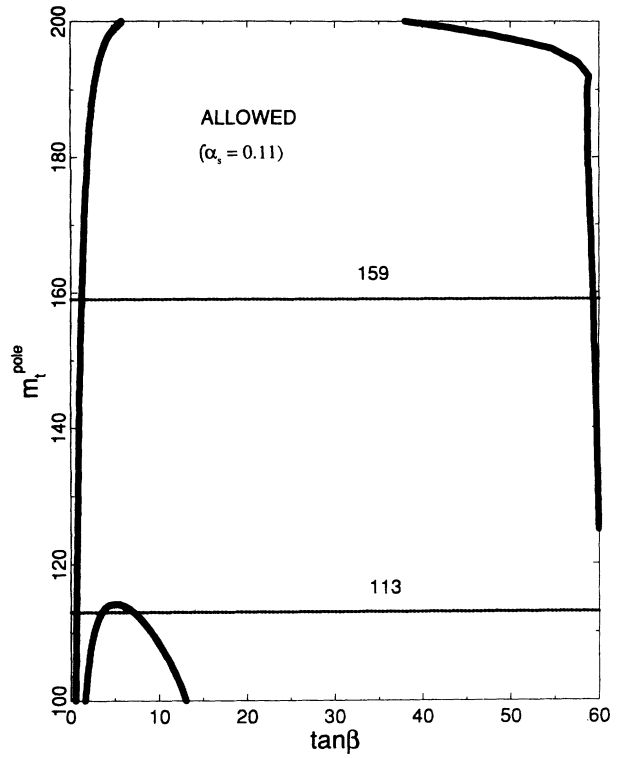

FIG. 5. The area in the m_t^{pole}-tanβ plane which is consistent with perturbative two-Yukawa unification and with $0.85 m_b^0(5\ \text{GeV}) < 4.45$ GeV assuming $\alpha_s(M_Z)=0.11$. The unification scale and α_G used in the calculation are those predicted by $\alpha_1-\alpha_2$ unification. We chose $\rho^{-1}=0.85$ for comparison with Figs. 2 and 3. m_t^{pole} is in GeV.

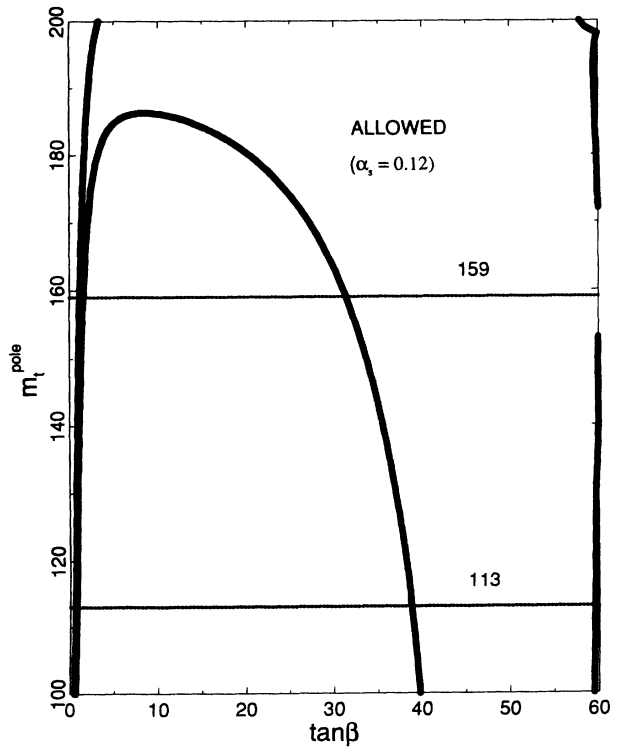

FIG. 6. The same as Fig. 5, except $\alpha_s(M_Z)=0.12$.

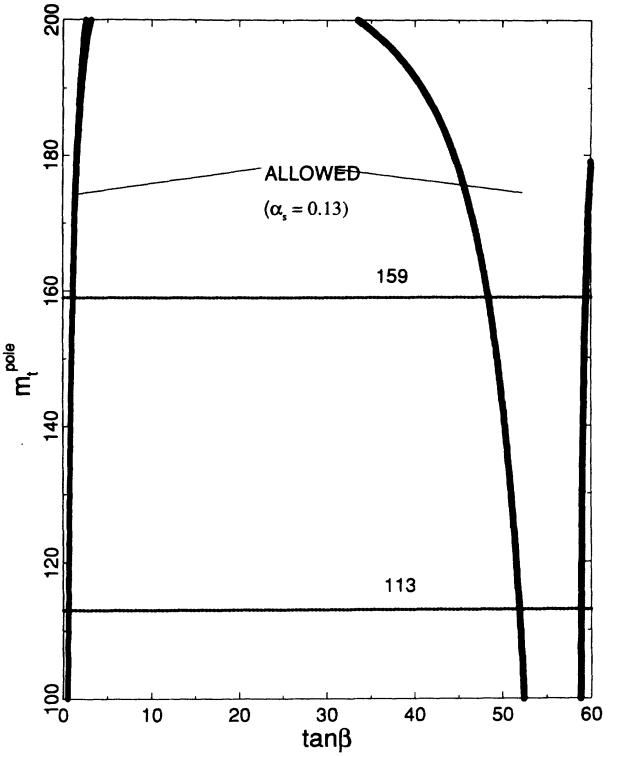

FIG. 7. The same as Fig. 5, except $\alpha_s(M_Z)=0.13$.

ished, and thus a given $h_\tau(M_G)=h_b(M_G)$ implies a lower $h_b(M_Z)$. However, the low value $\alpha_s(M_Z)=0.11$ requires large corrections to the coupling constant unification.

The above discussion also explains the slight differences between our results and those of previous analyses. Requiring (i) and using (2) for $s^2(M_Z)$ imply that $\alpha_s(M_Z)$ grows with m_t^{pole} [4], e.g., $\alpha_s(M_Z)\sim 0.12$ for $m_t^{pole}\sim 100$ GeV, and $\alpha_s(M_Z)\sim 0.13$ for $m_t^{pole}\sim 180$ GeV (see Fig. 1). Indeed, Fig. 2 roughly coincides with Fig. 6 for the former and with Fig. 7 for the latter. $h_t(M_Z)$ in (10)$\sim m_t^{pole}/\sin\beta$, but is diminished by (the m_t^{pole} dependent) $\alpha_s(M_Z)$. These all affect the balance between positive and negative contributions to the Yukawa coupling RGE's (i.e., the fixed points), and thus modify the $h_b(M_Z)$ prediction and increase the upper bound on m_t^{pole}.

IV. THE CORRECTION TERMS

We now turn to a detailed discussion of the correction parameter, ρ^{-1}. The coupling constant two-loop RGE's are solvable analytically, and it is convenient to write [39]

$$\frac{1}{\alpha_i(M_Z)}=\frac{1}{\alpha_G}+b_i t+\theta_i+H_i-\Delta_i \quad \text{for } i=1,2,3\ , \qquad (14)$$

where

$$t=\frac{1}{2\pi}\ln\frac{M_G}{M_Z}\approx 5.3$$

is the relevant scale parameter, and $\alpha_G\approx\frac{1}{24}$ is the coupling constant at the unification point, M_G. $b_i=6.6$, 1,

-3, for $i=1,2,3$, respectively, are the one-loop β-function coefficients; $\theta_i \approx 0.7$, 1.1, 0.6, for $i=1,2,3$, are the two-loop corrections; H_i are negligible Yukawa coupling two-loop contributions; and the functions Δ_i incorporate all other corrections to the calculation of order of magnitude consistent with θ_i. In our scheme, α_1 and α_2 are inputs. By taking linear combinations we obtain three predictions: i.e.,

$$\alpha_s(M_Z)=\alpha_s^0(M_Z)[\alpha_1,\alpha_2,\theta_i] + [\alpha_s^0(M_Z)]^2\Delta_{\alpha_s}[\Delta_1,\Delta_2,\Delta_3] , \tag{15a}$$

$$\frac{1}{\alpha_G}=\frac{1}{\alpha_G^0}[\alpha_1,\alpha_2,\theta_1,\theta_2]+\Delta_{\alpha_G}[\Delta_1,\Delta_2] , \tag{15b}$$

$$t=t^0[\alpha_1,\alpha_2,\theta_1,\theta_2]+\Delta_t[\Delta_1,\Delta_2] , \tag{15c}$$

where we explicitly separated the two-loop predictions with no corrections ($\Delta_i=0$) from the contribution of the correction functions, Δ_i. The expressions for Δ_{α_s}, Δ_{α_G}, and Δ_t are given in Appendix A.

The integration of the two-loop RGE's for the Yukawa couplings [36] is rather complicated and has to be done numerically. To estimate the theoretical correction terms it is useful to display the (one-loop) RGE's, i.e.,

$$\frac{dy_\alpha}{y_\alpha}=\left[\sum_{i=1,2,3} b_{\alpha;i}\alpha_i+\sum_{\beta=t,b,\tau} b_{\alpha;\beta}y_\beta+\cdots\right]dt' , \tag{16}$$

where $y_\alpha=h_\alpha^2/4\pi$ for $\alpha=t,b,\tau$; $t'=(1/2\pi)\ln(\mu'/M_Z)$; and we have omitted higher-order terms. $b_{b;i}=-\frac{7}{15}$, -3, $-\frac{16}{3}$, for $i=1,2,3$, respectively; and $b_{b;\beta}=1,6,1$, for $\beta=t,b,\tau$. ($b_{\tau;i}=-\frac{9}{5},-3,0$; $b_{\tau;\beta}=0,3,4$; $b_{t;i}=-\frac{13}{15}$, -3, $-\frac{16}{3}$; and $b_{t;\beta}=6,1,0$.) The balance between the negative $b_{\alpha;i}\alpha_i$ and the positive $b_{\alpha;\beta}y_\beta$ terms determines the infrared fixed point in the Yukawa coupling renormalization flow [24]. From (16) we obtain

$$h_b(M_G)=h_b(M_Z)\prod_{i=1}^{3}\left[\frac{\alpha_i^{\rm OL}(M_G)}{\alpha_i^{\rm OL}(M_Z)}\right]^{b_{b;i}/2b_i} F_b\Theta_b\rho_b , \tag{17}$$

and similarly for $h_\tau(M_G)$. The $\alpha_i^{\rm OL}$ are the one-loop (OL) couplings [i.e., $\theta_i=H_i=0$ in (14)]. Substituting instead two-loop (TL) (or input) expressions one has to compensate by properly modifying the two-loop correction Θ_b. F_b is the correction due to the non-negligible Yukawa contribution at one loop, i.e., $\int b_{\alpha;\beta}y_\beta dt'$. ρ_b incorporates the theoretical uncertainties in the RG calculation.

From (17) and the equivalent expression for h_τ [and assuming $h_b(M_G)=h_\tau(M_G)$] we have

$$m_b(M_Z)=m_\tau(M_Z)\left[\frac{\alpha_3^{\rm OL}(M_Z)}{\alpha_G^{\rm OL}}\right]^{8/9}\left[\frac{\alpha_1^{\rm OL}(M_Z)}{\alpha_G^{\rm OL}}\right]^{10/99} \times F^{-1}\Theta^{-1}\rho^{-1} , \tag{18}$$

where $F=F_b/F_\tau$, $\Theta=\Theta_b/\Theta_\tau$, and $\rho=\rho_b/\rho_\tau$. Setting $\Theta=\rho=1$, substituting the one-loop expressions for α_i and α_G, and assuming negligible Yukawa couplings (i.e., $F\approx 1$) gives an exact well-known one-loop expression. F^{-1} can be estimated analytically for $h_t \gg h_b$, h_τ [40]: i.e.,

$$F^{-1}\approx[1+11h_t^2(M_G)]^{-1/12} , \tag{19}$$

which gives $F^{-1}\sim 0.68$ for $h_t(M_G)\sim 3$. In general, however, a numerical analysis is required to fully incorporate $(F,\Theta)\neq 1$. The $m_b^0(M_Z)$ that we calculate is given by (18) with $\rho^{-1}=1$ and numerical values for F and Θ.

Before we turn to a rather technical derivation of the correction parameter ρ^{-1}, let us discuss a simple toy model and point out the ways in which it gets complicated. If the ideal desert and unification assumptions hold, then (neglecting two-loop terms)

$$\frac{1}{\alpha_1(M_Z)}=\frac{1}{\alpha_G^0}+b_1t^0 , \tag{20a}$$

$$\frac{1}{\alpha_2(M_Z)}=\frac{1}{\alpha_G^0}+b_2t^0 , \tag{20b}$$

$$\frac{1}{\alpha_s^0(M_Z)}=\frac{1}{\alpha_G^0}+b_3t^0 . \tag{20c}$$

We use (20a) and (20b) to define α_G^0 and t^0 in terms of the (input) $\alpha_{1,2}(M_Z)$. We now turn on the Δ_1 and Δ_2 correction functions and assume that no other corrections contribute to ρ^{-1}. The coupling constants are now given by

$$\frac{1}{\alpha_1(M_Z)}=\frac{1}{\alpha_G^0}+b_1t^0+\Delta_{\alpha_G}+b_1\Delta_t-\Delta_1 , \tag{21a}$$

$$\frac{1}{\alpha_2(M_Z)}=\frac{1}{\alpha_G^0}+b_2t^0+\Delta_{\alpha_G}+b_2\Delta_t-\Delta_2 , \tag{21b}$$

$$\frac{1}{\alpha_s(M_Z)}=\frac{1}{\alpha_s^0(M_Z)}-\Delta_{\alpha_s} =\frac{1}{\alpha_G^0}+b_3t^0+\Delta_{\alpha_G}+b_3\Delta_t . \tag{21c}$$

Δ_{α_G} and Δ_t are determined by the condition $\Delta_{\alpha_G}+b_i\Delta_t-\Delta_i=0$ for $i=1,2$, while (in the present approximation) Δ_{α_s} is due entirely to the change in α_G and t, i.e., $-\Delta_{\alpha_s}=\Delta_{\alpha_G}+b_3\Delta_t$. Also,

$$\frac{1}{\alpha_3(M_G)}=\frac{1}{\alpha_G^0}+\Delta_{\alpha_G} , \tag{22}$$

and the α_3 term in (18) now reads

$$\left[\frac{\alpha_s^0(M_Z)}{\alpha_G^0}\right]^{8/9}\{1+\tfrac{8}{9}[\alpha_s^0(M_Z)\Delta_{\alpha_s}+\alpha_G^0\Delta_{\alpha_G}]\} . \tag{23}$$

We thus obtain (in the toy model)

$$\rho^{-1}=\exp\{\tfrac{8}{9}[(\alpha_s^0(M_Z)-\alpha_G^0)\Delta_{\alpha_s}-b_3\alpha_G^0\Delta_t]\} . \tag{24}$$

In a more general case $\Delta_3\neq 0$ and $-\Delta_{\alpha_s}=\Delta_{\alpha_G}+b_3\Delta_t-\Delta_3$, where $\Delta_3=\Delta_3^{\rm SUSY}+\Delta_3^{\rm heavy}+\Delta_3^{\rm NRO}$ (for the low-scale threshold, high-scale threshold, and NRO contributions, respectively). NRO's ($\Delta_3^{\rm NRO}$) modify only the α_3 value and not any RGE coefficients (see Ref. [4] and below) and can be easily incorporated in our toy model, i.e., (24) is still correct if $-\Delta_{\alpha_s}=\Delta_{\alpha_G}+b_3\Delta_t-\Delta_3^{\rm NRO}$. The high-scale thresholds are more complicated because they not only affect

$\alpha_s(M_Z)$ but also change the β-function coefficient b_3 and the coefficient of the RGE for y_b (the $b_{b;3}$) at the various thresholds. The expression for ρ^{-1} will be derived below. Ignoring for now the threshold changes in $b_{b;3}$ the Δ_3^{heavy} contribution to $\rho^{-1}\sim\exp\{\frac{8}{9}[\alpha_s(M_Z)-\alpha_G]\Delta_3^{\text{heavy}}\}$, i.e., only the shift in $\alpha_s(M_Z)$, which affects the entire t' range in (16), is relevant. The effect of the change in b_3 above the threshold is of second order because it only affects a small region of the t' integral. Similarly, the leading contribution of Δ_3^{SUSY} is $\rho^{-1}\sim\exp\{\frac{8}{9}[\alpha_s(M_Z)-\alpha_3(\sim 1\ \text{TeV})]\Delta_3^{\text{SUSY}}\}$, which is a second order in small quantities (because it only affects a small region of the t' integral) and is therefore negligible.

Hence, the corrections to gauge couplings lead to

$$\rho^{-1}=\exp\{\tfrac{8}{9}[(\alpha_s(M_Z)-\alpha_G)\Delta'_{\alpha_s}-b_3\alpha_G\Delta_t]\}\ , \qquad (25)$$

where $-\Delta'_{\alpha_s}=-\Delta_{\alpha_s}+\Delta_3^{\text{SUSY}}=\Delta_{\alpha_G}+b_3\Delta_t-\Delta_3^{\text{NRO}}-\Delta_3^{\text{heavy}}$ includes all the shifts in $\alpha_s(M_Z)$ except those induced by Δ_3^{SUSY}. The additional corrections associated with the changes in $b_{b;3}$ at thresholds will be discussed below.

A different complication is due to the non-negligible role of the Yukawa couplings. F is modified when thresholds are decoupled. In particular, once the heavy Higgs doublet is decoupled the Yukawa operators and their evolution are modified. [Recall that we assume that we have one heavy ($M_H\gg M_Z$) Higgs doublet that decouples with the sparticles, and another light ($m_h\sim M_Z$) SM-like doublet that is responsible for all fermion masses.] Also, $h_\alpha(M_G)>1$ near either the h_t (low-tanβ) or h_b (large-tanβ) fixed points, and the most significant high-scale effect of correcting $t^0\to t^0+\Delta_t$ is due to the large Yukawa couplings and not to the $\alpha_G\Delta_t$ term. We will therefore treat high-scale Δ_t effects (ρ_t^{-1}) separately from Δ_{α_s} and Δ_{α_G} effects. Δ_{α_s} will include Δ_3 contributions which will be partially canceled by decoupling thresholds from both the α_3 and y_b RGE's. Thus, Δ_{α_s} and Δ_{α_G} effects will be described by $\rho_{\alpha_3}^{-1}$, which we derive first. (Using the input value of α_1, $\rho_{\alpha_1}^{-1}\sim 1$—see below.) We will then consider corrections to F (ρ_F^{-1}). Lastly, we will derive ρ_t^{-1} and rewrite ρ^{-1} in a way that reflects the correlations among $\rho_{\alpha_3}^{-1}$, ρ_F^{-1}, and ρ_t^{-1}. We will also comment on the role of the high-scale corrections, the case of using $\alpha_s(M_Z)$ as an input, and on corrections to the h_t/h_b ratio.

Allowing a complicated threshold structure near M_Z (and/or near M_G) gives a modified one-loop expression for m_b:

$$m_b(M_Z)=m_\tau(M_Z)\prod_{i=1}^{3}\prod_{k=0}^{n-1}\left[\frac{\alpha_i(\mu^k)}{\alpha_i(\mu^{k+1})}\right]^{(b^k_{b;i}-b^k_{\tau;i})/2b^k_i}F^{-1}(1+\Delta_F)\ , \qquad (26)$$

where k runs over the various thresholds; i.e., $\mu^0=M_Z$ and $\mu^n=M_G$. b^k is the one-loop coefficient of the respective RGE between μ^k and μ^{k+1}; and Δ_F represents the threshold corrections to F. By expanding (26) around (18) [in a similar way to (23)] and using the results of Ref. [4] we can obtain an approximate expression for ρ^{-1}. This yields better insight into the role of the different correction parameters than purely numerical estimates.

The important effects of the coupling constant uncertainties are in the α_3 terms. α_2 (in our approximation[11]) drops out from (26) and the residual uncertainties from α_1 are small when the input value is used. Recall that our strategy is to use the experimental values of $\alpha_1(M_Z)$ and $\alpha_2(M_Z)$ to predict α_3. The dominant corrections to the m_b prediction are the uncertainties in α_G and t due to Δ_1 and Δ_2, and the explicit uncertainties in Δ_3 (as was illustrated by our toy model). The latter can be divided into low-scale (Δ_3^{SUSY}) and to high-scale ($\Delta_3^{\text{heavy}}+\Delta_3^{\text{NRO}}$) contributions. The low-scale uncertainties have only a small effect on m_b because they only affect a small t' range in (16) (see the toy model). High-scale corrections affect the entire t' range. They modify both $\alpha_s(M_Z)$ (high-scale contributions to Δ_3 constitute a part of Δ_{α_s}) and either the β_3 function near M_G (Δ_3^{heavy}) or the $\alpha_3(M_G)$ value (Δ_3^{NRO}). All (high- and low-scale threshold) corrections to β_3 affect the α_3 terms in (26).

We denote the heavy X and Y vectors, color-triplet, and the adjoint color-octet, SU(2)-triplet (and singlet) superfield thresholds by M_V, M_5, and M_{24}, respectively. Some of the high-scale thresholds are strongly constrained by proton decay; i.e., in the minimal SU(5) model (which we assume) $M_5\sim M_G$ and perturbative consistency constrains $M_G\lesssim 3M_V$ [8,9]. $M_{24}\ll M_G$ is possible, and Δ_t is this scenario can be $\sim+0.5$ and the constraints on M_5 are relaxed (i.e., $M_5\gtrsim 0.1M_G$) [9]. Also, proton decay constraints can be removed by a simple modification of the model [41].

The sparticles and the Higgs doublet decouple from the α_i RGE at an effective scale, M_i, defined in Ref. [4] (see also Carena *et al.* [23]), i.e.,

$$\sum_\zeta\frac{b_i^\zeta}{(2\pi)}\ln\frac{M_\zeta}{M_Z}=\frac{b_i^{\text{MSSM}}-b_i^{\text{SM}}}{(2\pi)}\ln\frac{M_i}{M_Z}\quad\text{for } i=1,2,3\ . \qquad (27)$$

[11]Once sparticles are decoupled the degeneracy among various operators is lifted, e.g., the gaugino-sfermion-fermion coupling is different from the respective gauge coupling and the Higgsino-sfermion-fermion Yukawa coupling is different from the Higgs-boson–fermion–fermion one (see, for example, Chankowski [37]). In (26) we ignored this effect, which is negligible for sparticles and the Higgs-doublet below the TeV scale.

The summation is over all relevant thresholds, i.e., sparticles and the heavy Higgs doublet, and b_i^ζ is the ζ-particle contribution to the respective β function. M_i can be split by a factor of a few. In general, M_1 grows most significantly with the scalar mass, M_3 with the gaugino mass, M_1 and M_2 grow the same with the Higgsino mass, and $M_2 \ll M_1$ and/or $M_2 \ll M_3$. M_1, M_2 and M_3 all appear in Δ_{α_s}, Δ_{α_G}, and Δ_t. On the other hand, once either the gluinos or the squarks are decoupled, all squark-gluino loops are eliminated and $b_{b;3}=b_{b;3}^{\rm SM}$ [37], and two other scales of relevance are (in the approximation of degenerate squark masses) $\underline{M_3}=\min(M_{\rm gluino},M_{\rm squark})$ and $\overline{M_3}=\max(M_{\rm gluino},M_{\rm squark})$. One has $M_3^2=\overline{M_3}\underline{M_3}$.

We consider high-scale thresholds and NRO's ($\sim[\alpha_s(M_Z)-\alpha_G]\Delta$), low-scale thresholds ($\sim[\alpha_s(M_Z)-\alpha_3(\sim 1\ \text{TeV})]\Delta$), and corrections to the coupling constant unification predictions for $\alpha_s(M_Z)$ and α_G. We will discuss corrections to F and to t below. A more detailed treatment of low-scale effects will be needed if either some of the spectrum parameters are better known or if one assumes sparticle thresholds above the TeV scale. We will take[12] $\mu^1=\underline{M_3}$, $\mu^2=\overline{M_3}$, $\mu^3=M_{24}$, and $\mu^4=M_5$. The couplings and coefficients [to be substituted in (26)] read

$$\alpha_3(\mu^0)=\alpha_s^0(M_Z)+[\alpha_s^0(M_Z)]^2\Delta_{\alpha_s}\ , \tag{28a}$$

$$[\alpha_3(\mu^1)]^{-1}=[\alpha_s^0(M_Z)]^{-1}-b_3^0 t_3-\Delta_{\alpha_s}\ , \tag{28b}$$

$$[\alpha_3(\mu^2)]^{-1}=[\alpha_s^0(M_Z)]^{-1}-b_3^0 t_3-b_3^1\delta t_3-\Delta_{\alpha_s}\ , \tag{28c}$$

$$[\alpha_3(\mu^3)]^{-1}=[\alpha_3(\mu^2)]^{-1}-b_3^2\ln\frac{M_{24}}{\overline{M_3}}=[\alpha_3(\mu^4)]^{-1} \tag{28d}$$

$$[\alpha_3(\mu^4)]^{-1}=(\alpha_G^0)^{-1}-b_3^4 t_5+\Delta_{\alpha_G}-\Delta_3^{\rm NRO}\ , \tag{28e}$$

$$[\alpha_3(\mu^5)]^{-1}=[\alpha_3(\mu^n)]^{-1}=(\alpha_G^0)^{-1}+\Delta_{\alpha_G}-\Delta_3^{\rm NRO}\ , \tag{28f}$$

$$b_3^0=b_3^{\rm SM}=-7, b_3^1=-5, b_3^2=b_3^{\rm MSSM} =-3, b_3^3=0, b_3^4=1\ , \tag{28g}$$

$$b_{b;3}^0=b_{b;3}^1=b_{b;3}^{\rm SM}=-8, b_{b;3}^2=b_{b;3}^3 =b_{b;3}^4=b_{b;3}^{\rm MSSM}=-\frac{16}{3}\ . \tag{28h}$$

$t_3=(1/2\pi)\ln(\underline{M_3}/M_Z)$, $\delta t_3=(1/2\pi)\ln(\overline{M_3}/\underline{M_3})$, and $t_5=(1/2\pi)\ln(\overline{M_5}/M_G)$. (We replaced $\alpha_{s,G}^{\rm OL}$ by the two-loop $\alpha_{s,G}^0$ which introduces a negligible inconsistency.) In the $[M_{24},M_5]$ interval we cannot use (26) because $b_3^3=0$, and instead we have $b_{b;3}^3\alpha_3(\mu^3)\int_{\mu^3}^{\mu^4}d\ln\mu'$, which contributes

$$-\frac{4}{3}\frac{\alpha_G}{\pi}\left[\ln\frac{M_{24}}{M_G}-\ln\frac{M_5}{M_G}\right]=\alpha_G[-\tfrac{8}{9}\Delta_3^{24}+\tfrac{8}{3}t_5]$$

to $\ln\rho^{-1}$.

We obtain [for the α_3 terms in (26)]

$$\left[\frac{\alpha_3^{\rm OL}(M_Z)}{\alpha_G^{\rm OL}}\right]^{8/9}\rho_{\alpha_3}^{-1}\ , \tag{29}$$

where

$$\rho_{\alpha_3}^{-1}\equiv\exp(\tfrac{8}{9}\alpha_s^0\Delta_{\alpha_s}+\tfrac{8}{9}\alpha_G^0\Delta_{\alpha_G}-\tfrac{20}{9}\alpha_s^0 t_3-\tfrac{4}{9}\alpha_s^0\delta t_3 -\tfrac{8}{9}\alpha_G^0 t_5-\tfrac{8}{9}\alpha_G^0\Delta_3^{24}-\tfrac{8}{9}\alpha_G^0\Delta_3^{\rm NRO}) \tag{30}$$

[α_s^0 is $\alpha_s^0(M_Z)$.]

α_1 (and α_2) uncertainties feed into Δ_{α_s}, Δ_{α_G}, and Δ_t (we discuss the latter below). There are also $\rho_{\alpha_1}^{-1}$ corrections from thresholds and NRO's analogous to (30) from the $[\alpha_1(M_Z)/\alpha_1(M_G)]^{10/99}$ factor. However, these are negligible ($\lesssim 1\%$ or $\rho_{\alpha_1}^{-1}\sim 1$) when the experimental input value for $\alpha_1(M_Z)$ is used. We take in (26) $\rho_{\alpha_1}^{-1}=1$. The α_1 term in (16) does, however, lead to a small contribution to the ρ_t^{-1} term.

Δ_{α_s}, Δ_{α_G}, $\Delta_3^{\rm NRO}$ and Δ_3^{24} are defined in Ref. [4] and are given in Appendix A for completeness. They involve the low- and high-scale mass parameters introduced above, as well as the NRO effective strength η. To leading order η is the only NRO free parameter and it incorporates the degrees of freedom associated with the strength, sign, scale, and normalization of the dimension-five operators

$$-\frac{1}{2}\frac{\eta}{M_{\rm Planck}}{\rm Tr}(F_{\mu\nu}\Phi F^{\mu\nu})\ ,$$

where $F_{\mu\nu}$ is the field strength tensor and Φ is the adjoint scalar field. The range $-10\lesssim\eta\lesssim 10$ suggested in Ref. [4] is constrained only by perturbative consistency of the analysis.

Threshold corrections also affect the one-loop contribution from the Yukawa sector, i.e., $F^{-1}\to F^{-1}(1+\Delta_F)$, and it is convenient to define

$$\rho_F^{-1}=1+\Delta_F\ . \tag{31}$$

F^{-1} is a correction term, but it can be as large as a $\sim 30\%$ correction (which, in fact, is responsible for the successful m_b prediction in the MSSM), and, as we shall show, $\Delta_F\approx 2\%-4\%$. $M_{24}\ll M_G$ will not contribute since the adjoint superfield couples (to one loop) to the Yukawa operators via its coupling to the Higgs doublets, which drops out from the ratio. However, new and large Yukawa couplings will (radiatively) increase $h_\alpha(\mu)$ and thus affect the infrared fixed points and the perturbative limit; i.e., they affect F_α rather than the ratio F. (Such an effect may shift the h_t and h_b divergence lines in Figs. 2–7 inwards towards each other.) New Yukawa operators (that do contribute to the ratio[13]) are also generated

[12]The generalization to $M_5<M_{24}$ is straightforward. The $M_V<M_G$ case is much more difficult to describe. The heavy X and Y supervectors couple to the SU(3)×SU(2)×U(1) Yukawa operators in a complicated way. However, $M_V\gtrsim\frac{1}{3}M_G$ and the effects cannot be large.

[13]Their effect can be estimated by observation of the SU(5) invariant operators, i.e., $F_b/F_\tau\to 1$ above M_5: (19) is slightly modified for $M_5<M_G$, and the divergence lines move slightly outwards.

if $M_5 < M_G$ (see, for example, Hisano *et al.* [9]). The exact magnitude of such effects will be determined by the details of the high-scale Lagrangian.

There are, however, low-scale corrections to F^{-1}. We naively change the Yukawa coupling RGE's below the heavy Higgs doublet threshold $[t_H = (1/2\pi)\ln(M_H/M_Z)]$ to those which are appropriate given the SM fermion spectrum with one SM-like Higgs doublet (for example, see Giveon *et al.* [22]). We will also neglect (near M_Z) $h_b \cos\beta$, $h_\tau \cos\beta \sim 0$. We obtain

$$\rho_F^{-1} = \exp\{[\tfrac{1}{2}y_t + \tfrac{3}{4}y_t \sin^2\beta]t_H\} , \tag{32}$$

where here y_t is taken at M_Z (or more correctly, between M_Z and M_H), and $t_H < 0.38$. ρ_F^{-1} increases m_b by slightly diminishing the effect of F^{-1} in (18). Note that the F behavior distinguishes the MSSM, where only h_b gets corrected (to one loop) by h_t, from the SM where all fermions couple to only one Higgs doublet, and both h_b and h_τ get corrected. For $h_t < 1.1$ (as is reasonable at the low scale) $\rho_F^{-1} \lesssim 1.04$, which is a naive overestimate. Including a $h_b(M_Z) - h_\tau(M_Z)$ ($\lesssim 0.4$) contribution can increase ρ_F^{-1} by less than $\sim 2\%$ (the upper bound is for a large $\tan\beta$). In most parts of the plane the correction is moderate; i.e., $\rho_F^{-1} \lesssim 1.02$ if either $\sin\beta \sim 0$ or $h_t \ll 1$. Let us stress that this is a somewhat naive description which gets complicated in many ways. For example, a light t squark and a light chargino will still couple to the SM-like effective Yukawa operators. Such effects will have to be accounted for if and when the spectrum is better known and a refined analysis is required.

Lastly, t (which is determined by $\alpha_1 - \alpha_2$ unification) can be corrected by either corrections to the coupling constant unification [see Eq. (A3)] or by a split between the coupling constant and Yukawa coupling unification points. In the latter case, from our definition of M_G, $\Delta_t < 0$ (and it is reasonable to take $\Delta_t \gg -1$). [Effects (e.g., NRO's) that may split $h_b(M_G)$ and $h_\tau(M_G)$ can be also expressed in terms of the split between the unification points, but then Δ_t has no fixed sign.] Taking the approximation that $\Delta_t \ll t$ so that $\alpha_i(t) \approx \alpha_i(t + \Delta_t)$, $h_t(t) \approx h_t(t + \Delta_t)$ we find

$$\rho_t^{-1} = \exp[(-\tfrac{1}{2}y_t + 2\alpha_G^0)\Delta_t] , \tag{33}$$

where y_t in (33) is taken at M_G, i.e., $y_t(M_G) = h_t^2(M_G)/4\pi$, and $h_b \approx h_\tau$ dropped out. For small values of $h_t(M_G)$, a longer running time reduces $h_b(M_G)$ [and thus, increases the predicted $h_b(M_Z)$] and vice versa. The situation reverses for $h_t(M_G) \gtrsim \sqrt{16\pi\alpha_G} \sim \sqrt{2}$.

Collecting our results, we have

$$\rho^{-1} = \rho_{\alpha_3}^{-1} \times \rho_F^{-1} \times \rho_t^{-1} \equiv \rho_Z^{-1} \times \rho_G^{-1} , \tag{34}$$

where

$$\rho_Z^{-1} = \left[\frac{M_1}{M_Z}\right]^{25C_1/28 + 25C_2/112 + 15C_8} \times \left[\frac{M_2}{M_Z}\right]^{-(25C_1/7 + 275C_2/112 + 25C_8)} \times \left[\frac{M_3}{\overline{M_Z}}\right]^{[C_1 + C_3 - C_4]} \times \left[\frac{\overline{M_3}}{M_Z}\right]^{C_1 + C_4} \times \left[\frac{M_H}{M_Z}\right]^{C_7} , \tag{35}$$

and

$$\rho_G^{-1} = \left[\frac{M_V}{M_G}\right]^{-(3C_1/7 - 37C_2/14 + 24C_8)} \times \left[\frac{M_{24}}{M_G}\right]^{-(3C_1/14 + 33C_2/28 - C_5 + 12C_8)} \times \left[\frac{M_5}{M_G}\right]^{9C_1/14 + C_2/28 + C_6 + 12C_8/5} \times (1 + [0.29C_1 + 0.24C_2 + C_8]\eta) , \tag{36}$$

represent the low-scale and high-scale corrections, respectively. The coefficients C_i are defined and estimated in Table I. Note that $C_1 + C_3 - C_4 = 0$; i.e., $\underline{M_3}$ drops out. This is because $\underline{M_3}$ is associated with the change in $\alpha_s(M_Z)$ due the threshold, which is a second-order effect (see the discussion above). The $\overline{M_3}$ dependence, on the other hand, is due to the change of the $b_{b;3}$ coefficient and is of first order. We used $M_3^2 = \overline{M_3}\,\underline{M_3}$ and added Δ_{α_G} and $\Delta_3^{\rm NRO}$ η terms.

It is instructive to rewrite (using Table I)

$$\rho_Z^{-1} \approx \left[\frac{M_1}{M_Z}\right]^{0.02} \left[\frac{M_2}{M_Z}\right]^{-0.08} \left[\frac{\overline{M_3}}{M_Z}\right]^{0.025} \left[\frac{M_H}{M_Z}\right]^{0.01} . \tag{37}$$

(Different values of C_7 and C_8 were averaged.) If the spectrum was all degenerate at $M_{\rm SUSY}$, then $\rho_Z^{-1} \sim (M_{\rm SUSY}/M_Z)^{-0.025} \gtrsim 0.94$. We can invert the logic and use (37) to define an effective scale that gives ρ_Z^{-1} correctly. For example, in Ref. [4] we defined an effective scale parameter $A_{\rm SUSY}$:

$$25\ln\frac{M_1}{M_Z} - 100\ln\frac{M_2}{M_Z} + 56\ln\frac{M_3}{M_Z} = -19\ln\frac{A_{\rm SUSY}}{M_Z} . \tag{38}$$

($A_{\rm SUSY}$ here is $M_{\rm SUSY}$ of Ref. [4], and we have changed notation in order to avoid confusion with other definitions of $M_{\rm SUSY}$.) $A_{\rm SUSY}$ gives correctly the corrections to the $\alpha_s(M_Z)$ [or $s^2(M_Z)$] prediction, but does not

TABLE I. The coefficients C_i are defined and estimated using $s^2(M_Z)=0.2324$, $\alpha_s^0=0.125$, and $\alpha_G^0=0.040$.

	Definition	Estimate	Comments
C_1	$\frac{8}{9}\alpha_s^0(M_Z)/\pi$	+0.035	
C_2	$-\frac{8}{9}\alpha_G^0/\pi$	−0.011	
C_3	$-\frac{10}{9}\alpha_s^0(M_Z)/\pi$	−0.044	
C_4	$-\frac{2}{9}\alpha_s^0(M_Z)/\pi$	−0.009	
C_5	$-\frac{4}{3}\alpha_G^0/\pi$	−0.017	$M_{24}<M_5$
C_6	$-\frac{4}{9}\alpha_G^0/\pi$	−0.006	$M_{24}<M_5$
		+0.010	$h_t\sim 0.8$, $\beta\sim\frac{\pi}{2}$
C_7	$\frac{1}{8}(2+3\sin\beta)y_t(M_Z)/\pi$	+0.008	$h_t\sim 1.1$, $\beta\sim 0$
		+0.019	$h_t\sim 1.1$, $\beta\sim\frac{\pi}{2}$
C_8	$\frac{5}{672}[-y_t(M_G)+4\alpha_G^0]/\pi$	+0.0002	$h_t\sim 1$
		−0.0013	$h_t\sim 3$

contain any information on the spectrum—it can be as low as a few GeV for sparticles $\gg M_Z$. (See also Carena *et al.* [23].) Here, we can similarly define

$$\rho_Z^{-1}=\left[\frac{B_{\rm SUSY}}{M_Z}\right]^{-19C_1/28-250C_2/112+C_3+C_7-10C_8}\sim\left[\frac{B_{\rm SUSY}}{M_Z}\right]^{-0.025}. \tag{39}$$

The slightly negative exponent implies in many cases (for nondegenerate spectra) $B_{\rm SUSY}\lesssim M_Z$ (i.e., $M_2<M_1$, $\overline{M_3}$, M_H usually implies $\rho_Z^{-1}\gtrsim 1$). $B_{\rm SUSY}\geq M_Z$ for a strongly degenerate spectrum. For the spectra of Ref. [5] we find $\rho_Z^{-1}\sim 1$ ($A_{\rm SUSY}\approx 32$ and 21 GeV, $B_{\rm SUSY}\approx M_Z$). Taking the limits of heavy gluinos and of a degenerate spectrum we find $0.94\lesssim\rho_Z^{-1}\lesssim 1.06$. Away from the limits $\rho_Z^{-1}\to 1$.

Similarly to (37) we can rewrite

$$\rho_G^{-1}\approx\left[\frac{M_V}{M_G}\right]^{-0.030}\left[\frac{M_{24}}{M_G}\right]^{-0.004}\left[\frac{M_5}{M_G}\right]^{0.015}(1+0.007\eta)\,. \tag{40}$$

A scenario in which $M_{24}\ll M_G$, $M_5\sim(0.1-0.5)M_G$, $M_V=M_G$, and $\eta\approx -10$ would give $\rho_G^{-1}\approx 0.9$. This scenario is also consistent with limits from proton decay [8,9]. Furthermore, NRO's contribute only negligibly to Δ_{α_G} and to Δ_t (unless one allows NRO effects to be very large [7,42]). $M_{24}\ll M_G$ on the other hand can increase t significantly, i.e., $M_G\lesssim 5\times 10^{17}$ GeV (which is the reason that we can have $M_5<M_G$). A large negative η maintains an acceptable value of $\alpha_s(M_Z)$ in such a scenario. Lifting proton decay constraints (e.g., see Ref. [41]), we can have $M_5\ll M_G$ and $\rho_G^{-1}\approx 0.8-0.9$. Taking these limits and that of a degenerate spectrum and a large positive η we obtain $0.8\lesssim\rho_G^{-1}\lesssim 1.1$.

The high-scale corrections to the coupling constant unification emerge as the leading contribution to $\rho^{-1}\neq 1$. We would like to stress that η is not just a new *ad hoc* parameter. Given the precision to which we know the low-scale observables, one cannot ignore the likely possibility of unknown physics at the high-scale where the (supergravity-induced) MSSM breaks down, and which is parametrized in terms of NRO's [whose form is defined in SU(5) models]. Furthermore, similar corrections may arise in supergravity from nonminimal (and nonuniversal) gauge kinetic functions (see, for example, Ref. [42]). Unfortunately, this, in turn, introduces some ambiguity in RG calculations (via high-scale boundary conditions). It should also be noted that adding large representations [13–16,20], e.g., 126 of SO(10), does not introduce (for nearly degenerate heavy components) large threshold corrections to $\alpha_s(M_Z)$ and t. This is because the decoupled heavy components constitute a nearly complete representation (which acts equally on all the b_i's). Thus, the threshold corrections in the minimal model give a good estimate of ρ_G^{-1} (in models with a GUT sector, which are the relevant ones for Yukawa unification). A model-independent treatment of high-scale threshold effects on coupling constant unification was given in Ref. [4]. The heavy Yukawa sectors of different models may affect the infrared fixed points differently.

An arbitrary splitting of the two unification points[14] induces a ~5% uncertainty. By combining all the contri-

[14]Such a perturbation may be required in order to explain the low-energy ratios of the Yukawa couplings of the two light families. As we commented above, a small correction to $h_b/h_\tau=1$ at M_G is equivalent to a small shift in the Yukawa coupling unification point.

butions in quadrature (as a guideline only) we obtain

$$0.80 \lesssim \rho^{-1} \lesssim 1.15 \ . \tag{41}$$

$\rho^{-1}=1\pm 0.1$ is thus a reasonable range, and $\rho^{-1}=1\pm 0.15$ (which we adopted) is somewhat more extreme, but well within the allowed range. We would like to stress that all ranges extracted here are a guideline only. This range, which is controlled by high-scale corrections, is still valid when the sparticle spectrum is explicitly calculated (and, e.g., decoupled numerically).

As we pointed out above, corrections that either change the prediction for $\alpha_s(M_Z)$ or the positive contribution to (16) from Yukawa terms, affect the infrared fixed points and can slightly shift the corresponding divergence lines in Figs. 2–7. They may also affect the upper bound on $m_t^{\rm pole}$, and thus they induce a $\sim\pm 10$ GeV uncertainty to the upper bound value. However, the corrected range remains $\gtrsim 200$ GeV (see also Barger *et al.* [18]). In particular, it is much higher than the upper bound suggested by precision data [see Eq. (5)].

We would also like to point out that if $\alpha_1(M_Z)$, $\alpha_2(M_Z)$, and $\alpha_3(M_Z)$ are all used as inputs, then one arbitrarily adjusts Δ_{α_s} so that $\alpha_s^0+(\alpha_s^0)^2\Delta_{\alpha_s}$ is fixed at some desired value. The coupling constants do not unify unless one consistently corrects α_G and t as well. However, such a procedure is a reasonable approximation if $\Delta_3^{\rm SUSY}$ is small (or is known and corrected for). In that case one can minimize the residual uncertainty by calculating $\alpha_3(M_G)$ from the input value of $\alpha_s(M_Z)$ and from M_G (M_G is calculated from $\alpha_1-\alpha_2$ unification). Then only ρ_t^{-1}, ρ_F^{-1}, and $b_{b;3}$ terms contribute to ρ^{-1} [i.e., one can obtain their contribution by setting $C_1=C_2\equiv 0$ in (35) and (36)], and the residual uncertainty is small. Some caution is, however, needed. The coupling constant unification constraints are not integral in such a procedure (e.g., compare Figs. 2 and 5). In particular, the correlation between $\alpha_s(M_Z)$ and m_t is not manifest. A large m_t value implies larger values of $\alpha_s(M_Z)$ or, alternatively, very large corrections to coupling constant unification. Also, only Δ_1, Δ_2, $\Delta_3^{\rm NRO}$, and $\Delta_3^{\rm heavy}$ can induce first-order corrections to m_b, and thus can be used to fix $\alpha_s(M_Z)$. [NRO's renormalize and split $\alpha_i(M_G)$, and thus honestly modify the boundary conditions. The simplest way to adjust the $\alpha_s(M_Z)$ prediction to a given input value is by adjusting η—i.e., $\eta\sim -10$ corrects the $\alpha_s(M_Z)$ prediction to $\alpha_s(M_Z)\sim 0.11$.] As was illustrated by our toy model, $\Delta_3^{\rm SUSY}$ contributes to Δ_{α_s} but does not affect m_b to first order in small terms. Thus, unless one knows and corrects for the $\Delta_3^{\rm SUSY}$ contribution to the input $\alpha_s(M_Z)$ one introduces a significant theoretical uncertainty. Lastly, the experimental uncertainty in $\alpha_s(M_Z)$ is large, and arbitrarily varying $\alpha_s(M_Z)$ in that range is not very instructive. Nevertheless, it is useful in demonstrating the role of $\alpha_s(M_Z)$ in predicting m_b, as we saw in Sec. III.

Finally, the three-Yukawa-coupling unification strip (see Fig. 2) has uncertainties in both the $\tan\beta$ and the $m_t^{\rm pole}$ ranges, coming from corrections to the h_b/h_τ and h_t/h_b ratios, respectively. To one loop $(h_t/h_b)\sim(\alpha_1^{\rm OL}/\alpha_G^{\rm OL})^{-1/33}(F_b/F_t)$ and any uncertainties in the α_1 term are negligible. However, variation of $-0.5\lesssim\Delta_t\lesssim 0.5$ generates $\sim\pm 2\%$ ($\sim\pm 8\%$) correction if $h_t\sim h_b\sim h_\tau\sim 1$ (~ 2), i.e., $(\rho_b/\rho_{\rm top})_t\sim e^{y_\alpha(M_G)\Delta_t/2}$. Additional uncertainty of

$$0.95\lesssim(\rho_b/\rho_{\rm top})_F\sim\exp\{[y_t(M_Z)-\tfrac{5}{2}y_b(M_Z)]t_H\}\lesssim 1$$

(we assume $\tan\beta\gg 1$) is associated with the decoupling of the heavy Higgs doublet. We estimate a $\sim\pm 5$–10% uncertainty in the $m_t^{\rm pole}$ range that corresponds to three-Yukawa unification.

V. CONCLUSIONS

Grand unified theories typically predict $h_b=h_\tau$ at M_G, and contain nonfundamental Higgs representations. These distinguish such models from some other realizations of the MSSM, e.g., string-inspired GUT-like models. Above, we explicitly embedded the MSSM in a minimal SU(5) model, and concluded that such a model is constrained to a small area of the parameter space. We showed that corrections to a two-loop calculation of the bottom mass (when assuming grand unification) are manifested in various ways. Parametrizing those corrections, we were able to relate them to the correction parameters identified in Ref. [4], and to study their magnitude and behavior in some detail. The theoretical uncertainty in the bottom mass prediction is typically $\lesssim 15\%$. We thus took (given the ambiguities in the extraction of m_b from experiment) $0.85m_b^0(5\ {\rm GeV})<4.45$ GeV as a (conservative) constraint. Requiring this, as well as requiring perturbative Yukawa couplings up to M_G and identifying the coupling constant and the (third-family) Yukawa coupling unification points, we found that the range $2.7\lesssim\tan\beta\lesssim 40$ is excluded (as well as $m_t^{\rm pole}\gtrsim 215$ GeV), and that, in agreement with other authors, the allowed area in the $m_t^{\rm pole}$-$\tan\beta$ plane is described by low- and high-$\tan\beta$ branches (where the former saturates the h_t fixed-point line). The separation between the two branches is determined by the correction factor. Requiring all three (third-family) Yukawa couplings to meet constrains 160 GeV $\lesssim m_t^{\rm pole}$ and requires a large $\tan\beta$. We demonstrated that the allowed parameter space grows for lower (input) values of $\alpha_s(M_Z)$, but that the MSSM prefers higher values. We further argued that the $s^2(M_Z)$ quadratic dependence on $m_t^{\rm pole}$ cannot be ignored as it correlates the $\alpha_s(M_Z)$ prediction with $m_t^{\rm pole}$, and thus affects the $m_t^{\rm pole}$ dependence of the m_b prediction, as well as the upper bound on $m_t^{\rm pole}$ and the range of $m_t^{\rm pole}$ for which intermediate values of $\tan\beta$ are allowed. Finally, we expect the above observations and radiative breaking of SU(2)×U(1) to have mutual implications, and suggest that the above constraint is still valid in a calculation in which the sparticle spectrum, and therefore ρ_Z^{-1}, is calculated explicitly. (The larger uncertainty in the calculation comes from the unification-scale physics rather than from the details of the sparticle spectrum.) Our hope is that a careful study of various correction terms will eventually result in reliable constraints on the MSSM parameter space, and in a way that can distinguish different real-

izations of the MSSM. Here we have showed (in agreement with others) that by measuring $\tan\beta$ one can exclude simple (and some extended) GUT structures at the high-scale.

ACKNOWLEDGMENT

This work was supported by the Department of Energy Grant No. DE-AC02-76-ERO-3071.

APPENDIX: THE CORRECTION FUNCTIONS

For completeness, we give the correction functions to the coupling constant unification [in the minimal SU(5) MSSM]. For more details, see Ref. [4]. Corrections that depend on $m_t^{\rm pole}$ or the conversion to the $\overline{\rm DR}$ scheme are included in the numerical procedure, and are not quoted below. All the parameters are defined above (see Sec. IV). The correction functions are

$$28\pi\Delta_{\alpha_s}=-12\ln\frac{M_V}{M_G}-6\ln\frac{M_{24}}{M_G}+18\ln\frac{M_5}{M_G}+25\ln\frac{M_1}{M_Z}-100\ln\frac{M_2}{M_Z}+56\ln\frac{M_3}{M_Z}+8.00\eta\ , \tag{A1}$$

$$-336\pi\Delta_{\alpha_G}=+888\ln\frac{M_V}{M_G}-396\ln\frac{M_{24}}{M_G}+12\ln\frac{M_5}{M_G}+75\ln\frac{M_1}{M_Z}-825\ln\frac{M_2}{M_Z}+50.0\eta\ , \tag{A2}$$

$$\frac{336\pi}{5}\Delta_t=-24\ln\frac{M_V}{M_G}-12\ln\frac{M_{24}}{M_G}+\frac{12}{5}\ln\frac{M_5}{M_G}+15\ln\frac{M_1}{M_Z}-25\ln\frac{M_2}{M_Z}+1.0\eta\ , \tag{A3}$$

$$\Delta_3^{24}=\frac{3}{2\pi}\ln\frac{M_{24}}{M_G}\ , \tag{A4}$$

$$\Delta_3^{NRO}\approx 0.03\eta\ . \tag{A5}$$

[1] See, for example, LEP Collaborations, Phys. Lett. B **276**, 247 (1992).

[2] J. Ellis, S. Kelley, and D. V. Nanopoulos, Phys. Lett. B **249**, 441 (1990); P. Langacker and M. Luo, Phys. Rev. D **44**, 817 (1991); U. Amaldi, W. de Boer, and H. Fürstenau, Phys. Lett. B **260**, 447 (1991); F. Anselmo, L. Cifarelli, A. Peterman, and A. Zichichi, Nuovo Cimento **104A**, 1817 (1991).

[3] S. Dimopoulos and H. Georgi, Nucl. Phys. **B193**, 150 (1981); N. Sakai, Z. Phys. C **11**, 153 (1981); E. Witten, Nucl. Phys. **B188**, 513 (1981). For reviews, see H. P. Nilles, Phys. Rep. C **110**, 1 (1984); in *Testing The Standard Model,* edited by M. Cvetič and P. Langacker (World Scientific, Singapore, 1991), p. 633; H. E. Haber and G. L. Kane, Phys. Rep. C **117**, 75 (1985); R. Barbieri, Riv. Nuovo Cimento **11**, 1 (1988); L. E. Ibáñez and G. G. Ross, in *Perspectives in Higgs Physics,* edited by G. L. Kane (World Scientific, Singapore, 1993).

[4] P. Langacker and N. Polonsky, Phys. Rev. D **47**, 4028 (1993).

[5] G. G. Ross and R. G. Roberts, Nucl. Phys. **B377**, 571 (1992). More recently, the Ross and Roberts analysis was extended to include dark-matter considerations by R. G. Roberts and L. Roszkowski, University of Michigan Report No. UM-TH-33/92, 1992 (unpublished).

[6] H. Georgi and S. L. Glashow, Phys. Rev. Lett. **32**, 438 (1974); H. Georgi, H. R. Quinn, and S. Weinberg, *ibid.* **33**, 451 (1974). For reviews, see P. Langacker, Phys. Rep. C **72**, 185 (1981); in *Proceedings of the Ninth Workshop on Grand Unification,* Aix les Bains, France, 1988, edited by R. Barloutaud (World Scientific, Singapore, 1988), p. 3; G. G. Ross, *Grand Unified Theories* (Benjamin, New York, 1984); R. N. Mohapatra, *Unification and Supersymmetry* (Springer, New York, 1986, 1992). See also Ref. [3].

[7] C. T. Hill, Phys. Lett. **135B**, 47 (1984); Q. Shafi and C. Wetterich, Phys. Rev. Lett. **52**, 875 (1984).

[8] R. Arnowitt and P. Nath, Phys. Rev. Lett. **69**, 725 (1992); Phys. Rev. D **46**, 3981 (1992).

[9] J. Hisano, H. Murayama, and T. Yanagida, Phys. Rev. Lett. **69**, 1014 (1992); Nucl. Phys. **402**, 46 (1993).

[10] For a recent review, see P. Langacker, University of Pennsylvania Report No. UPR-0539T, 1992 (unpublished).

[11] R. Barbieri and L. J. Hall, Phys. Rev. Lett. **68**, 752 (1992); L. J. Hall and U. Sarid, *ibid.* **70**, 2673 (1993).

[12] M. S. Chanowitz, J. Ellis, and M. K. Gaillard, Nucl. Phys. **B128**, 506 (1977); A. J. Buras, J. Ellis, M. K. Gaillard, and D. V. Nanopoulos, *ibid.* **135**, 66 (1978).

[13] H. Fritzsch, Phys. Lett. **70B**, 436 (1977); **73B**, 317 (1978); Nucl. Phys. **B155**, 189 (1979); H. Georgi and C. Jarlskog, Phys. Lett. **86B**, 297 (1979).

[14] S. Dimopoulos, L. J. Hall, and S. Raby, Phys. Rev. Lett. **68**, 1984 (1992); Phys. Rev. D **45**, 4192 (1992); **46**, 4793 (1992); **47**, R3697 (1993); V. Barger, M. S. Berger, T. Han, and M. Zralek, Phys. Rev. Lett. **68**, 3394 (1992); G. W. Anderson, S. Rabi, S. Dimopoulos, and L. J. Hall, Phys. Rev. D **47**, R3702 (1993).

[15] K. S. Babu and Q. Shafi, Bartol Report No. BA-92-27, 1992 (unpublished); Phys. Rev. D **47**, 5004 (1993); Phys. Lett. B **311**, 172 (1993).

[16] G. Giudice, Mod. Phys. Lett. A **7**, 2429 (1992); H. Dreiner, G. K. Leontaris, and N. D. Tracas, National Technical University Report No. NTUA 33/92, 1992 (unpublished); G. K. Leontaris and N. D. Tracas, Report No. NTUA 37/92, 1992 (unpublished).

[17] H. Arason, D. J. Castaño, E. J. Piard, and P. Ramond, Phys. Rev. D **47**, 232 (1993).

[18] V. Barger, M. S. Berger, and P. Ohmann, Phys. Rev. D **47**, 1093 (1993); V. Barger, M. S. Berger, P. Ohmann, and R. J. N. Phillips, Phys. Lett. B **314**, 351 (1993).

[19] S. G. Naculich, Phys. Rev. D **48**, 5293 (1993).

[20] K. S. Babu and R. N. Mohapatra, Phys. Rev. Lett. **70**,

2845 (1993).
[21] J. Ellis and M. K. Gaillard, Phys. Lett. **88B**, 315 (1975).
[22] B. Ananthanarayan, G. Lazarides, and Q. Shafi, Phys. Rev. D **44**, 1613 (1991); M. Bando, T. Kugo, N. Maekawa, and H. Nakano, Mod. Phys. Lett. A **7**, 3379 (1992); H. Arason *et al.*, Phys. Rev. Lett. **67**, 2933 (1991); A. Giveon, L. J. Hall, and U. Sarid, Phys. Lett. B **271**, 138 (1991); S. Kelley, J. L. Lopez, and D. V. Nanopoulos, Phys. Lett. B **274**, 387 (1992). For discussion of the nonsupersymmetric case, see, for example, P. H. Frampton, J. T. Liu, and M. Yamaguchi, *ibid.* **277**, 130 (1992).
[23] M. Carena, S. Pokorski, and C. E. M. Wagner, Nucl. Phys. **B406**, 59 (1993); M. Olechowski and S. Pokorski, *ibid.* **B404**, 590 (1993). (Note the different notation; e.g., their T_i is our M_i.)
[24] B. Pendleton and G. G. Ross, Phys. Lett. **98B**, 291 (1981); C. T. Hill, Phys. Rev. D **24**, 691 (1981).
[25] W. A. Bardeen, A. J. Buras, D. W. Duke, and T. Muta, Phys. Rev. D **18**, 3998 (1978), and references therein. For the weak angle definition, see A. Sirlin, Phys. Lett. B **232**, 123 (1989); S. Fanchiotti and A. Sirlin, Phys. Rev. D **41**, 319 (1990); A. Sirlin, Nucl. Phys. **B332**, 20 (1990), and references therein.
[26] G. Degrassi, S. Fanchiotti, and A. Sirlin, Nucl. Phys. **B351**, 49 (1991).
[27] S. Bethke and S. Catani, in *QCD and High Energy Hadronic Interactions,* Proceedings of the 27th Rencontre de Moriond, Les Arcs, France, 1992, edited by J. Tran Tranh Van (Editions Frontières, Gif-sur-Yvette, 1992).
[28] P. Langacker, University of Pennsylvania Report No. UPR-0555T, 1993 (unpublished).
[29] P. Langacker and N. Polonsky, University of Pennsylvania Report No. UPR-0594T, 1993 (unpublished).
[30] N. Gray, D. J. Broadhurst, W. Grafe, and K. Schilcher, Z. Phys. C **48**, 673 (1990).
[31] For a recent review of various observables, SM RGE's, β and γ functions, see H. Arason *et al.*, Phys. Rev. D **46**, 3945 (1992). Note that some values used there, i.e., those for $\alpha_s(M_Z)$ and m_τ, are different from ours, and that the authors follow Narison [34] in their definition of m_b.
[32] H. Marsiske, in *Proceedings of the Second Workshop on Tau Lepton Physics,* Columbus, Ohio, 1992, edited by K. K. Gan (World Scientific, Singapore, 1992), p. 1.
[33] J. Gasser and H. Leutwyler, Phys. Rep. C **87**, 77 (1982).
[34] S. Narison, Phys. Lett. B **197**, 405 (1987); **216**, 191 (1989).
[35] W. Siegel, Phys. Lett. **84B**, 193 (1979); D. M. Capper, D. R. T. Jones, and P. van Nieuwenhuizen, Nucl. Phys. **B167**, 479 (1980); I. Antoniadis, C. Kounnas, and K. Tamvakis, Phys. Lett. **119B**, 377 (1982).
[36] J. E. Björkman and D. R. T. Jones, Nucl. Phys. **B259**, 533 (1985).
[37] P. H. Chankowski, Phys. Rev. D **41**, 2877 (1990).
[38] For a recent discussion, see, for example, M. Drees and M. M. Nojiri, Nucl. Phys. **B369**, 54 (1992). A scenario with $h_t \approx h_b$ was considered by M. Olechowski and S. Pokorski, Phys. Lett. B **214**, 393 (1988). See also Ref. [23].
[39] L. Hall, Nucl. Phys. **B178**, 75 (1981); M. B. Einhorn and D. R. T. Jones, *ibid.* **B196**, 475 (1982).
[40] L. E. Ibáñez and C. López, Nucl. Phys. **B233**, 511 (1984).
[41] L. E. Ibáñez and G. G. Ross, Nucl. Phys. **B368**, 3 (1992).
[42] J. Ellis *et al.*, Phys. Lett. **155B**, 381 (1985); M. Drees, *ibid.* **158B**, 409 (1985).